

Transition metal atomic multiplets in the ligand K-edge x-ray absorption spectra and multiple oxidation states in the L_{2,3} emission of strongly correlated compounds

J. Jiménez-Mier, P. Olalde-Velasco, W.-L. Yang, and J. Denlinger

Citation: [AIP Conference Proceedings](#) **1607**, 39 (2014); doi: 10.1063/1.4890701

View online: <http://dx.doi.org/10.1063/1.4890701>

View Table of Contents: <http://scitation.aip.org/content/aip/proceeding/aipcp/1607?ver=pdfcov>

Published by the [AIP Publishing](#)

Articles you may be interested in

[In-operando synchronous time-multiplexed O K-edge x-ray absorption spectromicroscopy of functioning tantalum oxide memristors](#)

J. Appl. Phys. **118**, 034502 (2015); 10.1063/1.4926477

[Restricted active space calculations of L-edge X-ray absorption spectra: From molecular orbitals to multiplet states](#)

J. Chem. Phys. **141**, 124116 (2014); 10.1063/1.4896373

[Fe K-edge X-ray absorption spectroscopy study of Pb\(Fe₂/3W₁/3\)O₃-PbTiO₃ multiferroic ceramics](#)

J. Appl. Phys. **113**, 114104 (2013); 10.1063/1.4795505

[Differences between L₃ and L₂ x-ray absorption spectra of transition metal compounds](#)

J. Chem. Phys. **101**, 6570 (1994); 10.1063/1.468351

[Relationship between the area of L_{2,3} x-ray absorption edge resonances and the d orbital occupancy in compounds of platinum and iridium](#)

J. Chem. Phys. **76**, 1451 (1982); 10.1063/1.443105

Transition Metal Atomic Multiplets in the Ligand K-Edge X-Ray Absorption Spectra and Multiple Oxidation States in the $L_{2,3}$ Emission of Strongly Correlated Compounds

J. Jiménez-Mier*, P. Olalde-Velasco^{†,**}, W. -L. Yang[†] and J. Denlinger[†]

**Instituto de Ciencias Nucleares, UNAM, 04510 México DF, México*

†The Advanced Light Source, Lawrence Berkeley Laboratory, Berkeley, CA 94720, USA

***Swiss Light Source. Paul Scherrer Institut, CH-5232 Villigen PSI, Switzerland*

Abstract. We present results that show that atomic multiplet ligand field calculations are in very good agreement with experimental x-ray absorption spectra at the $L_{2,3}$ edge of transition metal (TM) di-fluorides (MF_2 , $M=Cr-Cu$). For chromium more than one TM oxidation state is needed to achieve such an agreement. We also show that signature of the TM atomic multiplet can be found at the pre-edge of the fluorine K-edge x-ray absorption spectra. TM atomic multiplet ligand field calculations with a structureless core hole show good agreement with the observed pre-edges in the experimental fluorine absorption spectra. Preliminary results for the comparison between calculated and experimental resonant x-ray emission spectra for nominal CrF_2 with more than one oxidation state indicate the presence of three chromium oxidation states in the bulk.

Keywords: Transition metal compounds, x-ray absorption and emission, oxidation states.

PACS: 32.80.Dz, 32.80.Fb

INTRODUCTION

Core level spectroscopies are well established tools to study the electronic structure of many interesting compounds [1]. X-Ray absorption spectroscopy (XAS) is ideally suited to investigate electronic states in the conduction band [1, 2], while x-ray emission spectroscopy (XES) gives information about electronic states in the valence band [1, 3]. In the soft x-ray region the electronic transitions follow the electric-dipole selection rules and therefore the electronic states probed are selected by the element and also by the orbital symmetry. This is particularly useful in the study of strongly correlated transition metal (TM) compounds. XAS and XES at the metal $L_{2,3}$ edge are direct probes of the 3d-projected valence and conduction bands, respectively. At the ligand K edge they probe the respective anion 2p-projected bands. The absorption spectra at the metal are quite sensitive to the atomic multiplet, ligand field effects and to the TM oxidation state. Some of these, characteristic of the transition metal, can be also found at the absorption and emission spectra at the ligand K edge. This is only possible because of the strong hybridization between the TM 3d (more localized) and 4s, p (more delocalized) orbitals in the valence and conduction bands [4, 5]. The signature of the TM 3d orbitals at the ligand K edge should be more visible in the transition metal difluorides, which are the most ionic of the TM compounds. The resonant emission spectra at the metal $L_{2,3}$ edge are also very sensitive to the atomic multiplet and ligand field interactions. They should also be sensitive to the TM oxidation state, but these kind of studies have only begun recently [6].

In this article we present experimental and theoretical results that shows evidence of the TM 3d and fluorine 2p orbital hybridization at the pre-edges of the fluorine K absorption spectra. The experimental pre-edges were isolated from the rest of the conduction band, and they resulted in well defined multiplets. These multiplets were then compared with the TM L_3 and L_2 absorption spectra and also with the result of an atomic multiplet calculation of the TM L-edge but with the 2p hole Coulomb and spin-orbit interaction removed.

We also present results of resonant x-ray emission of CrF_2 . This is the only transition metal difluoride for which a single ionization state atomic multiplet calculation is not in agreement with the experimental data. We showed recently that much better agreement can be found by including three chromium oxidation states (Cr^+ , Cr^{2+} , and Cr^{3+}) in the calculation [5]. In this work we pursue this analysis further by exploring the possibility of finding these oxidation states also in resonant emission. To accomplish this, the results of the atomic multiplet calculation were used to generate resonant emission spectra for each oxidation state, using the same parameters that gave such a good agreement with

the XAS data. A preliminary analysis shows that the same three oxidation states are present in resonant emission spectra. These results for emission indicate that the three oxidation states are present in the sample bulk, as opposed to the total electron yield XAS measurements [5] that are surface sensitive.

EXPERIMENT

Fresh commercially available polycrystalline MF_2 ($\text{M} = \text{Cr} - \text{Zn}$) from Sigma Aldrich with nominal purity greater than 99.9 % were prepared inside a N_2 flow bag and introduced inside the UHV experimental chamber. All x-ray absorption and emission measurements took place at beamline 8.0.1 of the Advanced Light Source in Berkeley. Details of the beamline are presented elsewhere [7]. Experimental x-ray absorption spectra were recorded in the total electron yield (TEY) mode. All XAS spectra presented in this work were recorded at room temperature. The resonant x-ray emission spectra were recorded in a soft x-ray fluorescence spectrometer, which is a grazing incidence instrument with a fixed entrance slit and a position sensitive area detector. Photon emission spectra are then recorded at selected values of the incoming photon energy by positioning the spectrometer detector along the Rowland circle to intercept the wavelength region of interest. The recorded emission spectra were corrected for self-absorption in the sample [8] considering that the sample holder normal made an angle of 45° with respect to both incoming and outgoing photon directions. The emission spectra are recorded in the so-called unpolarized geometry [9].

LIGAND FIELD MULTIPLY CALCULATIONS

Atomic multiplet calculations including ligand field effects (LFM) in D_{4h} symmetry were performed to reproduce metal $L_{2,3}$ edges XAS spectra. The ligand field parameters $10Dq$, Ds , and Dt , the contraction factor for the atomic Slater integrals, and the monochromator width were all varied until we found the best agreement with measured metal XAS $L_{2,3}$ edges [10, 11]. Our approach successfully accounts for the main structures found at the TM $L_{2,3}$ edges in all the series [5]. For CrF_2 three ionic states, namely Cr^+ , Cr^{2+} , and Cr^{3+} , were included in the calculation [5]. This allows for the possibility of sample oxidation and/or disproportionation. The resulting spectrum is then the linear superposition of the individual spectra that gives the best agreement with experiment [5]. Because the calculated spectra are normalized to the number of 3d holes, the superposition coefficients directly give the ratio of that ionic state present in the sample [2, 11].

The intra-atomic multiplet structure is calculated in terms of the Slater integrals [12]. These are reduced from their Hartree-Fock values to take into account some degree of electron-electron correlation [12]. For our compounds ligand field effects are given by the $10Dq$, Ds and Dt parameters, where $10Dq$ is the energy splitting of a 3d orbital in octahedral (O_h) symmetry, and Ds and Dt indicate deviations from O_h symmetry [10]. Values for the $2p_j$ core hole widths required to perform the calculations were taken directly from the article by Krause and Oliver [13].

Resonant emission spectra for CrF_2 were calculated using the Kramers-Heisenberg expression [8]. The output from the ligand field multiplet calculation provides the state energies and the electric dipole transition matrix elements between the $2p^6 3d^n$ (initial and final) and the $2p^5 3d^{n+1}$ (intermediate) configurations. The calculation includes the effect of random orientations of the polycrystalline sample, full interference effects, but was carried out for an emission direction along the magic angle [8]. These calculations were repeated for the three chromium oxidation states found in the XAS spectrum. The coefficients of a direct linear superposition of each emission spectrum were then varied until the best agreement with experiment was obtained.

RESULTS AND DISCUSSION

Transition metal multiplet effects at the fluorine absorption edge

The atomic multiplet calculation gives very good results for the $L_{2,3}$ absorption spectra of the MF_2 ($\text{M} = \text{Cr} - \text{Ni}$) compounds [5]. In the case of chromium we had to consider three metal oxidation states, namely Cr^+ , Cr^{2+} and Cr^{3+} . On the other hand, the fluorine K edge absorption spectra give important information about the hybridization between the fluorine 2p and transition metal unoccupied orbitals [4, 5]. The fluorine K-edge XAS has broad features above 687 eV, common to all the series, that result from hybridization between fluorine 2p and TM 4s, 4p orbitals. At the low

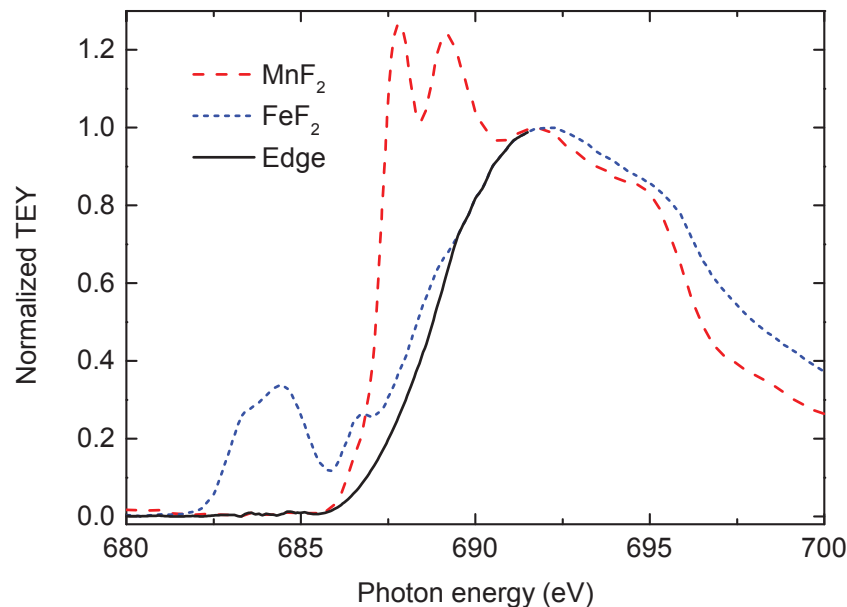


FIGURE 1. Procedure to isolate the pre-edge of the fluorine K edge x-ray absorption. Dashed line (red online): normalized MnF_2 XAS; short dashed line (blue online): normalized FeF_2 XAS; continuous line (black): edge that is used for subtraction. For an explanation of the subtraction procedure see the text.

energy end of this broad feature one finds narrow peaks characteristic of each compound, that constitute the pre-edge. Below this energy there are sharp pre-edges, characteristic of the TM, that correspond to excitation into states resulting from an admixture of fluorine 2p and TM 3d orbitals. In general there is more than one narrow peak at the pre-edges, which can be taken as an indication that the TM 3d multiplet also has an effect at the fluorine K absorption edge. This becomes more apparent when one subtracts a broad edge, common to all compounds, that is the onset of the F 2p and TM 4s, 4p hybridized band. In Fig. 1 we show how this edge is determined [5]. First, all spectra are normalized so that they had the same intensity at the local maximum at about 691 eV. On the low energy side, below 685 eV, the edge was chosen as the lowest points of the absorption spectra, which belong to MnF_2 . In the region between 688 and 691 eV the edge is given by the lowest points of the absorption spectra, which now correspond to FeF_2 . Finally, the edge values between 685 and 688 eV were obtained by a cubic spline interpolation connecting these low and high energy segments. The same broad edge was subtracted to the fluorine XAS to isolate the pre-edges for the other difluorides [5].

Once the pre-edge peaks for each compound are isolated, one can compare it with the multiplet structures found at both the L_3 and L_2 edges of the corresponding transition metal. For this comparison we shifted the TM L-edges so that there was a correspondence between features (peaks and shoulders) at the fluorine pre-edge and corresponding features at the metal edges. Notice that we could have also shifted the F K edge to the TM L_3 , L_2 edges. The result of this comparison for CoF_2 is shown in Fig. 2. There is a good correspondence between features in both Co $L_{2,3}$ and F-K spectra. The cobalt L_3 edge has several well defined peaks that give a clear indication of the multiplet structure. These peaks can be aligned under a broad fluorine K pre-edge structure. The high energy shoulders at L_3 also seem to align with the structures on the raising 4s,4p band, especially at about 690 eV. The cobalt L_2 edge is broadened by a Coster-Kronig process responsible for the nonradiative decay of the $2p_{1/2}$ hole [14]. But even here the broad peak and its high energy shoulder seem to align with features at the fluorine pre-edge. The same type of analysis can be carried out for the other members of the MF_2 difluoride family [5]. In general one can establish a one to one correspondence between the metal $L_{2,3}$ features and peaks and shoulders at the isolated fluorine K pre-edge in all members of the family [5].

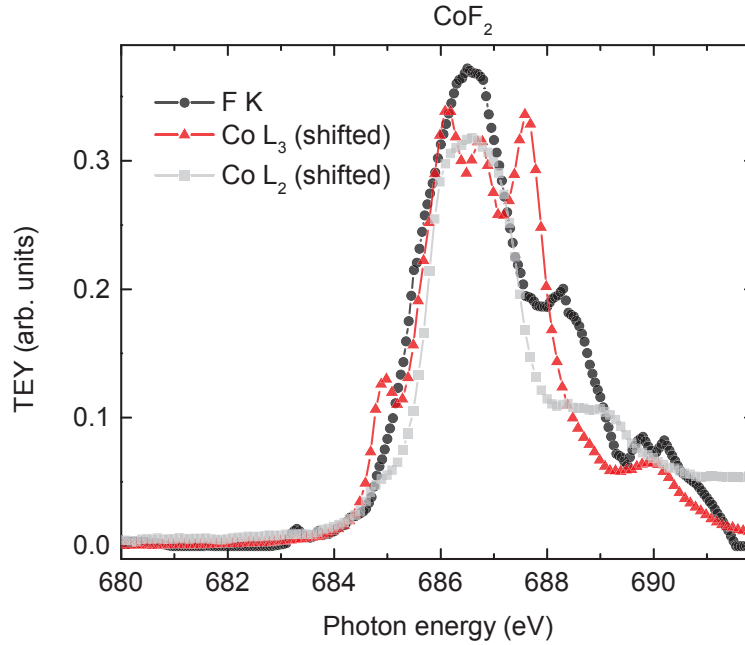


FIGURE 2. Comparison between the fluorine pre-edge structure and the *shifted* transition metal L_3 and L_2 absorption edges for CoF_2 . The fluorine edge is shown with dots, the TM L_3 are the triangles (red online) and the TM L_2 edges are the squares (gray online). The intensities of all spectra were adjusted to make the comparison easier to the eye.

However, in all cases the TM $L_{2,3}$ absorption edges are also affected by the multiplet structure of the $2p_j$ core hole in the metal, and the fluorine K pre-edge corresponds to the production of a $1s$ core-hole in fluorine. Therefore, it is important to perform a calculation that removes the $2p_j$ core hole multiplet effects.

We performed calculations of $2p$ to $3d$ absorption spectra with a $2p$ hole that does not interact with the $3d$ subshell and has no $2p$ spin-orbit interaction. We will refer to this $2p$ hole as a *2p structureless hole*. Technically, in the calculations we used the same parameters obtained to reproduce metal $L_{2,3}$ XAS spectra in Ref. [5], but we set the values of the Slater $F^k(2p; 3d)$ and $G^k(2p; 3d)$ integrals responsible for the $2p$ - $3d$ Coulomb interaction and the metal $2p$ spin-orbit interaction equal to zero. The results are x-ray absorption spectra corresponding to the $2p \rightarrow 3d$ excitation in the metal, but containing only the multiplet structure of the $3d^{n+1}$ subshell in the presence of a structureless hole. Thus, the relative positions of the features in these simulated spectra give the multiplet structure of the $3d^{n+1}$ configuration. In Fig. 3 we show an example of such a calculation for CoF_2 . In the bottom panel we show the $2p \rightarrow 3d$ transitions that resulted from the ligand field multiplet calculation for the cobalt $L_{2,3}$ edges that, once convoluted with core-hole Lorentzians and an instrument Gaussian, gave such a good agreement with the experimental spectrum in Ref. [5]. The top panel gives the transitions that are obtained with the structureless $2p$ hole calculation. Because we turned off the $2p$ spin-orbit interaction there is no splitting between L_2 and L_3 . Also the multiplet structure is modified because of the absence of the $2p$ - $3d$ Coulomb interaction. The transition lines of this structureless core hole calculation were obtained in terms of the atomic reduced matrix element $\langle 2p || r || 3d \rangle$. They have to be convoluted with a Lorentzian to take into account the width of the F $2p$ band, and also with an instrument Gaussian function. The resulting calculated $3d^{n+1}$ absorption spectrum is then shifted in order to compare with the corresponding fluorine K XAS pre-edge. This procedure was repeated for all the other TM difluorides.

A comparison between the isolated pre-edge and the structureless hole XAS calculation for MnF_2 , FeF_2 and CoF_2 is shown in Fig. 4. The calculated transitions indicated by vertical bars were convoluted with the same Lorentzian and Gaussian profiles that were used to reproduce the TM $L_{2,3}$ absorption edges in Ref. [5]. For MnF_2 we see that the d^{5+1} calculation for Mn^{2+} shows two main structures which once shifted resemble nicely the experimentally observed

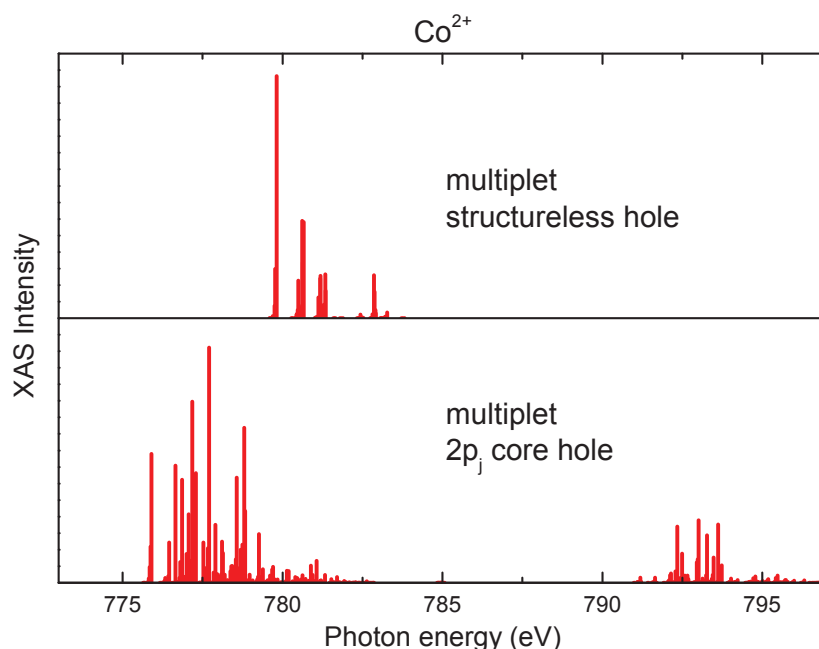


FIGURE 3. Comparison between a ligand field multiplet calculation for CoF_2 with a structureless $2p$ core hole (top panel) and the normal calculation with full interaction with the $2p$ hole (bottom panel). The plot only give the energies and relative intensities of the calculated transitions. Each line must then be convoluted with Lorentzian and Gaussian broadening functions to be able to compare with experimenta spectra. For details see the text.

doublet. In the case of FeF_2 , we present a d^{6+1} calculation for Fe^{2+} . It clearly predicts the number of structures and accounts relatively well for their energy separation but fails in reproducing their relative intensity. For CoF_2 , the results for a d^{7+1} configuration in Co^{2+} are shown. Here the calculation predicts four main structures. The first two seem to match the F-K pre-edge while the third and fourth may be obscured by the rising of the Co $4s$, $4p$ band. The same kind of agreement between experimental pre-edge data and structureless core hole calculations is found for the other members of the TM difluoride family [5]. This is the case even for CrF_2 for which the calculation has to include, once again, three oxidation states. In most of the cases the calculation correctly accounts for the number of structures but slightly fails in estimating the energy separation among them and their relative intensity as compared to those observed in the spectra. This result is surprising considering the simplistic model followed in this work to capture evidence of the $\text{TM}3d\text{-F}2p$ hybridization process. In this description, during the x-ray absorption at the F-K edge, a $1s$ F electron is promoted to F $2p$ unoccupied states. Once in the $2p$ conduction band, due to hybridization, there is a probability that this electron will be partially localized in the vicinity of the $3d$ sub-bands. Because of this, aside from the attractive effect of the F $1s$ core hole left behind, this electron will experience the interactions inherent to $3d$ shell electrons: Coulomb $3d\text{-}3d$, $3d\text{-spin}$ orbit, as well as the crystal field exerted by surrounding F ions. Therefore, by the x-ray absorption process at the F-K edge we are actually indirectly probing the $3d$ shell and the interaction that $3d$ electrons experiment by the inclusion of an extra $3d$ electron.

Oxidation states in the chromium L resonant emission spectra of CrF_2

Here we present preliminary results for chromium resonant x-ray emission that indicate the presence of different oxidation states in the bulk of a CrF_2 sample. On the experimental side, we used the TEY spectrum at the chromium $L_{2,3}$ edges to select excitation energies at which we recorded resonant emission spectra. The same TEY spectrum

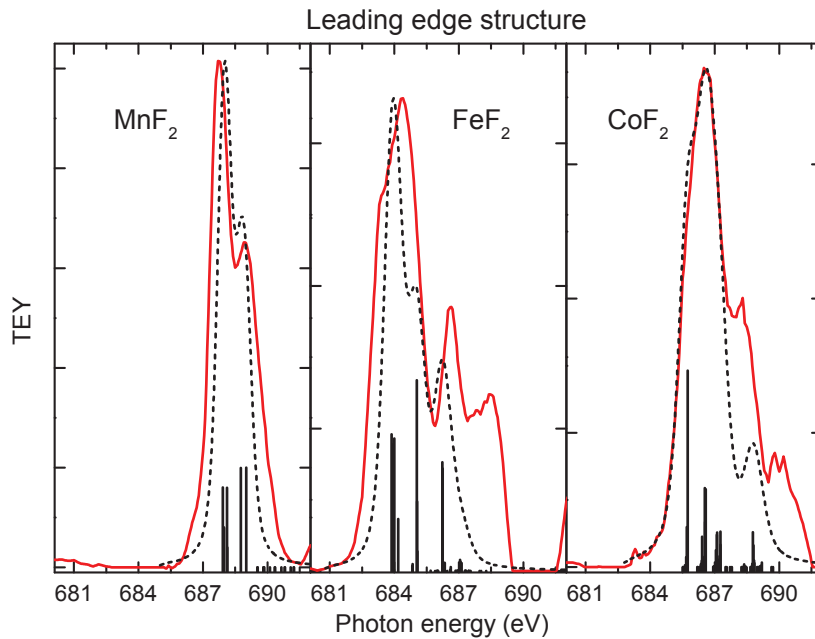


FIGURE 4. Comparison between the experimental fluorine pre-edge spectra and the result of the structureless 2p hole calculation for the MF_2 ($M = \text{Mn, Fe and Co}$). Continuous line (red online) are the experimental spectra. The calculated transitions are the vertical bars and the convoluted spectra are the dashed lines.

was also used to establish the presence of different oxidation states in the sample [5]. The results of the ligand field multiplet calculation that was used for this purpose are shown in Fig. 5, where we present the relative contribution of each oxidation state and the sum. The symbols are the values of the excitation energy that were used for the emission spectra. Using the same parameters we calculated, with the Kramers-Heisenberg expression [3, 8], the corresponding emission spectra for each oxidation state. Therefore, we are making a Resonant Inelastic X-Ray Scattering (RIXS) analysis that probes the same oxidation in the initial and final states, including dd excitations in the TM. To the best of our knowledge, studying TM oxidation states with RIXS has only begun recently [6].

It would be tempting to take linear combinations of these individual emission spectra, with the same coefficients that were used in the TEY data, to calculate the emission of multiple oxidation states. However, this is not possible because the relative contributions in emission are strongly dependent of the penetration depths of both incoming and outgoing photons in the sample. Both of these are strongly modulated by the relative absorption cross section at the excitation energy. We therefore decided to calculate, for a given value of the excitation energy, emission spectra for each oxidation state, and then calculate the coefficients of the linear superposition that gave the best agreement with the experimental data. This is relatively straightforward in the region of the L_3 edge. For larger values of the excitation energy there is one more complication because the emission data also have features resulting from filling a $2p_{3/2}$ that is nonresonantly produced. The calculation is not capable of reproducing this *normal emission peak* (see Fig. 6).

In Fig. 6 we make a comparison between the experimental and calculated resonant emission spectra recorded at the two values of the excitation energy indicated by (e) and (k) in Fig. 5. These correspond, respectively, to the maximum of L_3 and L_2 . The experimental and calculated spectra are shown at the top panels of Fig. 6. Both experimental spectra have features in common. The narrow peak at the high energy end is the elastic peak. It corresponds to photons emitted with the same energy of the photons used for excitation. Towards lower energy the elastic peak is followed by a series of peaks and shoulders that correspond to dd excitations that originate from the decay into excited states of the chromium $3d^n$ configuration. Finally, a broad peak to the low energy side corresponds to normal emission. It cannot be predicted by our resonant calculation. There is reasonable agreement between experiment and theory for these two

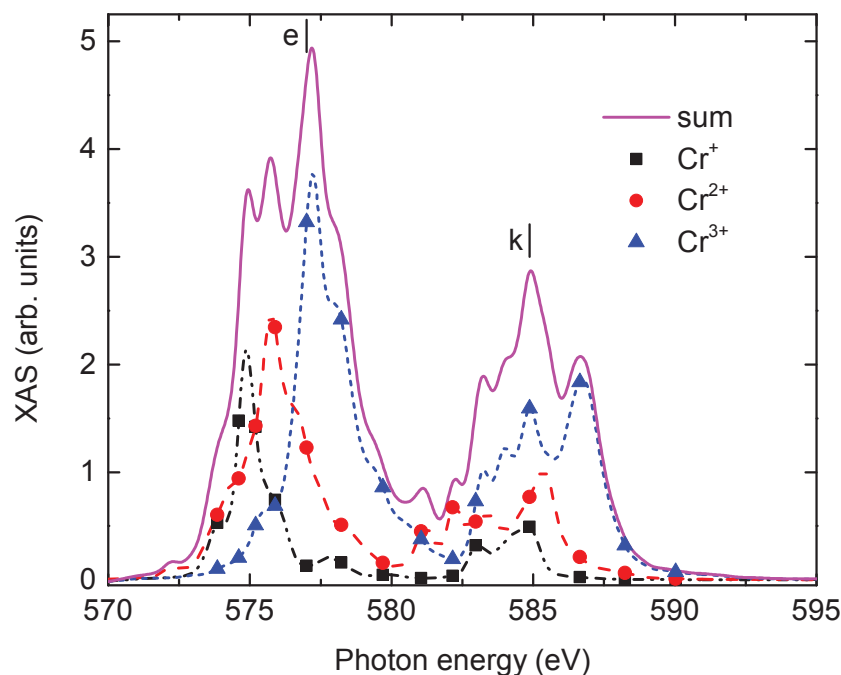


FIGURE 5. Contribution of the three oxidation states to the calculated $L_{2,3}$ absorption spectrum of CrF_2 . The symbols give the excitation energies at which we recorded emission spectra. The squares (black online) correspond to Cr^+ , the bullets (red online) to Cr^{2+} and the triangles (blue online) to Cr^{3+} . The vertical lines labelled (e) and (k) give the excitation energies used to obtain the emission spectra shown in Fig. 6.

spectra. In (e) both experiment and theory are dominated by a sharp elastic peak, followed by narrow inelastic emission and a low energy shoulder at about 571 eV. However, the energy separation between the main two peaks is larger in the calculation. Theory also predicts a small peak just above 570 eV that is also present, though with less intensity, in the experimental spectrum. There is also good agreement between experiment and theory for spectrum (k). However, the elastic peak is stronger in the calculation, and the energy difference with respect to the inelastic features is smaller in the experiment. Theory predicts two low energy peaks at 576 and 578 eV that seem to be present as shoulders to the high energy side of the normal emission peak.

The bottom panels of Fig. 6 give the contributions of each oxidation state (Cr^+ , Cr^{2+} and Cr^{3+}) to the calculated emission. Their relative intensities were chosen to give the best agreement with the experiment. It is remarkable that the three oxidation states are present in both spectra, and that the contribution from Cr^{3+} is the smallest. However, no quantitative information can be extracted at this point because these emission spectra are affected by the relative transition matrix elements and also, as it was already discussed, by the penetration depth of incoming and outgoing photons.

CONCLUDING REMARKS

In this paper we presented the results of a detailed study of the fluorine K pre-edge of the MF_2 ($M = \text{Cr} - \text{Ni}$) transition metal difluorides. We showed that it is possible to isolate this pre-edge from the contribution of the broad 4s, 4p band common to all members of the family. A direct comparison between the TM $L_{2,3}$ and fluorine K edges indicates that there is evidence of the TM $3d^{n+1}$ multiplet structure at the fluorine pre-edge. A multiplet calculation that follows a

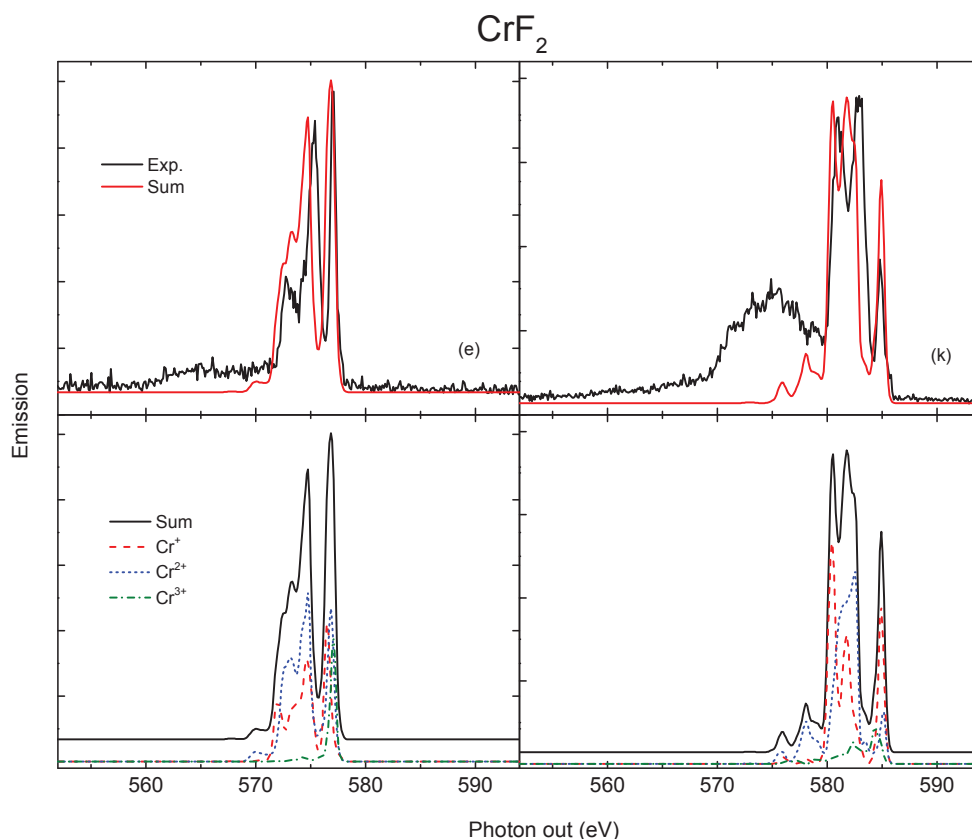


FIGURE 6. Contribution of the chromium ionization states to emission at excitation energies (e) and (k) in Fig. 5. The bottom panels give the contribution of each oxidation state and their sum and the top panels show the comparison of the sum with the experimental spectra.

rather simplistic model is in agreement with the experimental results, even for the relative intensities of the absorption peaks that are calculated using the TM $2p \rightarrow 3d$ transition matrix elements.

We also showed that the chromium resonant x-ray emission of CrF_2 confirms the presence of Cr^+ , Cr^{2+} and Cr^{3+} observed in XAS. The experimental data are in good agreement with linear superpositions of ligand field multiplet calculations of these oxidation states. However, further analysis is needed to assess whether it is possible to use this information to make quantitative determinations about the relative content of these oxidation states.

ACKNOWLEDGMENTS

The Advanced Light Source is supported by DOE(DE-AC03-76SF0009). This work was supported by CONACyT México under research grant No. 56764. POV would like to thank postdoctoral support from CONACyT under the agreement 0166436 and from the ALS scientific support group.

REFERENCES

1. F. M. F. de Groot, and A. Kotani, *Core Level Spectroscopy of Solids*, CRC Press, Reading, Massachusetts, 2008.
2. J. Stöhr, *NEXAFS Spectroscopy*, Springer, 1992.
3. L. J. P. Ament, M. van Veenendaal, T. P. Devereaux, J. P. Hill, and J. van den Brink, *Rev. Mod. Phys.* **83**, 705–767 (2011).
4. P. Olalde-Velasco, J. Jiménez-Mier, J. D. Denlinger, Z. Hussain, and W. L. Yang, *Phys. Rev. B* **83**, 248002 (2011).
5. P. Olalde-Velasco, J. Jimenez-Mier, J. Denlinger, and W. L. Yang, *Phys. Rev. B* **87**, 245136 (2013).
6. M. M. van Schooneveld, E. Suljoti, C. Campos-Cuerva, R. W. Gosselink, A. M. J. van der Eerden, J. Schlappa, K. J. Zhou, C. Monney, T. Schmitt, and F. M. F. de Groot, *The Journal of Physical Chemistry Letters* **4**, 1161–1166 (2013).
7. J. J. Jia, T. A. Callcott, J. Yurkas, A. W. Ellis, F. J. Himpsel, G. Samant, J. Stöhr, D. L. Ederer, J. A. Carlisle, E. A. Hudson, L. J. Terminello, D. K. Shuh, and R. C. C. Perera, *Rev. Sci. Instrum.* **66**, 1394 (1995).
8. J. Jiménez-Mier, G. M. Herrera-Pérez, P. Olalde-Velasco, D. L. Ederer, and T. Schuler, *Rev. Mex. Fís.* **54**, 30–35 (2008).
9. Y. Harada, and S. Shin, *J. Electron Spectrosc. Relat. Phenom.* **136**, 143 (2004).
10. F. de Groot, *Coord. Chem. Rev.* **249**, 31–63 (2005).
11. E. Stavitski, and F. M. F. de Groot, *Micron* **41**, 687 (2010).
12. R. D. Cowan, *The Theory of Atomic Structure and Spectra*, University of California Press, Ltd., Berkeley, 1981.
13. M. O. Krause, and J. H. Oliver, *J. Phys. Chem. Ref. Data* **8**, 329 (1979).
14. R. Brydson, L. A. J. Garvie, A. J. Craven, H. Sauer, F. Hofer, and G. Cressey, *J. Phys.: Condens. Matter* **5**, 9379 (1993).